Journal of Thermal Analysis and Calorimetry (2021) 146:1629–1639
https://doi.org/10.1007/s10973-020-10170-7

Chitosan-regulated inorganic oxyacid salt flame retardants: preparation and application in PVC composites

Qingyi Song[1] · Hongjuan Wu[2] · Hao Liu[1] · Tian Wang[1] · Weihua Meng[1] · Hongqiang Qu[1]

Received: 11 December 2019 / Accepted: 4 August 2020 / Published online: 12 August 2020

Abstract

A series of chitosan-modified inorganic oxyacid salt flame retardants (IOS-CS) were synthesized and used as flame retardants to improve the fire resistance of poly(vinyl chloride) (PVC) composites while improving the mechanical properties of the materials. The thermal stability of the material was analyzed by TG test; the flame-retardant and smoke suppression properties were evaluated by limiting oxygen index (LOI) and cone calorimeter test, and the mechanical properties were analyzed by tensile test and impact test. The TG results showed that the addition of flame retardant can promote the early cross-linking decomposition of PVC composites, not only advance the decomposition temperature of the material but also promote the formation of char layer and increase the char residual content. LOI and cone calorimeter test results showed that stannate chitosan (Sn-CS) can improve flame retardant and smoke suppression more effectively than other samples. Compared with pure PVC, the addition of Sn-CS increased its LOI from 26.6 to 30.5% and reduced the total heat release value and total smoke release by 18.23% and 52.55%, respectively. At the same time, the addition of the flame retardants had no large deterioration effect on the mechanical properties of the material. The tensile properties of flame-retardant PVC were slightly reduced compared with pure PVC, and the impact resistance was even improved to some extent.

Keywords Flame retardant · Smoke suppression · Bio-based · Mechanical properties

Introduction

Poly(vinyl chloride) (PVC) is one of the largest polymer materials in the world in terms of production and use [1, 2]. It is widely used in daily necessities, wire and cable, pipe and building materials and plays a vital role in the history of polymer applications [3–5]. PVC materials have good flame-retardant properties due to their high chlorine content [6]. However, some additives are often added during the processing, which has a certain impact on the flame-retardant and smoke suppression properties of PVC materials [7]. Therefore, it is meaningful to study the flame retardant and smoke suppression of PVC composites.

Traditional inorganic flame retardants including inorganic compounds, metal hydroxides and complexes have been widely used in PVC composites due to their high stability, low toxicity and low cost [8–10]. However, traditional inorganic flame retardants generally have low flame-retardant efficiency, which need large quantity of addition to meet the flame-retardant demand of high-grade materials. For example, the metal hydroxide represented by magnesium hydroxide (MDH) is a common kind of flame retardant for PVC composites. However, the large addition of MDH leads to a decrease in the mechanical properties of the substrate, difficulty in processing and a significant deterioration in mechanical properties, electrical properties and physical properties [11–13].

Common methods for solving the problem of inorganic flame retardants include synergistic flame retardancy, ultrafine and surface modification [14–16]. Zhang et al. [17] prepared a multilayer microcapsule flame retardant with core–shell structure using zinc stannate, aluminum hydroxide and melamine–formaldehyde resin. Experiments showed

✉ Hongqiang Qu
hqqu@163.com

[1] Engineering Technology Research Center for Flame Retardant Materials and Processing Technology of Hebei Province, Key Laboratory of Analytical Science and Technology of Hebei Province, College of Chemistry and Environmental Science, Hebei University, Baoding 071002, People's Republic of China

[2] Department of Foundation Couses, Agricultural University of Hebei, Cangzhou 061100, People's Republic of China

that the flame retardant can effectively increase the limiting oxygen index (LOI) of PVC materials and significantly reduce its smoke emission. Moreover, the addition of melamine–formaldehyde resin has significantly improved the mechanical properties of composite materials. Wang et al. [18] synthesized a nano-graphene oxide/α-zirconium phosphate hybrid (GOZP) by an in situ method, which not only made RPVC foam exhibit good flame retardancy, but also endowed it with high mechanical properties. In addition, some novel methods have been applied to the modification of inorganic flame retardants, such as layer self-assembly and microcapsule methods. However, these improvements also have problems such as high cost and complicated processes. Therefore, the development of high-efficiency and comprehensive performance of PVC flame-retardant smoke-eliminating system still has the significance of further research.

In view of environmental considerations, researchers have recently noticed the possibility of bio-based substances as flame retardants. Chitosan (CS) is an amino polysaccharide having a polyhydroxy and amino structure, and this makes it easy to react with other compounds [19, 20]. In addition, the materials have the advantages of low cost, easy degradation and non-toxicity, which make it a good choice for preparing flame retardants [21, 22]. Therefore, we can molecularly design CS according to the flame-retardant requirements. Zhang et al. [23] prepared a novel CS-based flame retardant containing phosphorus, nitrogen and carbon by reacting phytic acid with CS. Applying this flame retardant to ethylene vinyl acetate copolymer (EVA) not only effectively reduces heat release, but also increases the Young's modulus of the material. This proves that CS has great research value in improving polymer materials.

In this study, a series of oxyacid salts containing CS cationic including chitosan stannate (Sn-CS), chitosan molybdate (Mo-CS), chitosan silicate (Si-CS) and chitosan tungstate (W-CS) were prepared by reacting acetic acid-dissolved CS with stannate, molybdate, silicate and tungstate, respectively. The flame retardants were applied to PVC composites. The thermal stability and flame-retardant properties of PVC composites were investigated by thermogravimetric analysis (TG) and cone test. Meanwhile, the mechanical properties of the composites were investigated by tensile test and impact test. This research will provide new insights into the design and preparation of bio-based inorganic flame retardants.

Experimental

Materials

Chitosan (CS, AR, deacetylation degree $\geq 95\%$) was acquired from Aladdin Chemistry Co., Ltd. (Shanghai, China). Sodium stannate trihydrate ($Na_2SnO_3{\cdot}3H_2O$, AR), sodium molybdate dihydrate ($Na_2MoO_4{\cdot}2H_2O$, AR), sodium silicate ($Na_2SiO_3{\cdot}9H_2O$, AR) and sodium tungstate dihydrate ($Na_2WO_4{\cdot}3H_2O$, AR) were obtained from Kemiou Chemistry Co., Ltd. (Tianjin, China). Acetic acid (CH_3COOH, AR) was obtained from Tianjin Damao Chemistry Co., Ltd. PVC (TL-1000, density D 1.35 g cm^{-3}, average polymerization degree K67) was supplied by Tianjin LG Dagu Chemical Co., Ltd. The lubricants calcium stearate and stearic acid were offered by Tianjin Branch of the USA and Europe Chemical Reagent Co., Ltd. Dioctyl phthalate (DOP, TP) and organotin stabilizer were supplied by Baoding Yisida Co., Ltd. Coupling agent (KH-550) was provided by Shanghai Guoyao Chemical Co., Ltd.

Synthesis of chitosan-modified inorganic oxyacid salt (IOS-CS)

Taking the preparation of Sn-CS as an example: First, 0.50 g of CS was stirred in 50 mL of deionized water for 1 h. 3.50 mL of glacial acetic acid was added to the CS suspension, and the stirring was continued for several hours to form a homogeneous solution. Then, 5.33 g of $Na_2SnO_3{\cdot}3H_2O$ was dissolved in 50 mL of deionized water and stirred until dissolved. Thereafter, the two of solutions were slowly added dropwise to the three-necked flask to which 50 mL of deionized water was preliminarily added. And stirring was continued. The batch was agitated at 80 °C for an additional 4 h and then cooled to room temperature. And then, the product was filtered, washed three times with deionized water and lyophilized for 24 h. Finally, Sn-CS was obtained, and the yield of the product is 86%. The Mo-CS, Si-CS and W-CS were prepared in the same way, and the yields are 75%, 80% and 82%, respectively.

Preparation of PVC/IOS-CS composites

The PVC composites consisted of 100 phr (per hundred resin) PVC resin, 40 phr DOP, 3 phr stabilizer, 1 phr silane coupling agent KH550, 0.5 phr calcium stearate, 0.5 phr stearic acid and 10 phr flame retardant. The mixture was then blended with a two-roll mill at 140 °C for 8 min. After this, the composites were transferred to a stainless steel mold, preheated at 170 °C for 3 min, pressed at 120 MPa for 5 min and cooled to room temperature at 120 MPa for 5 min.

Characterization

The morphology of the char residues was measured by scanning electron microscopy (SEM, JSM-7500, JEOL) with the acceleration voltage of 15 kV.

The crystal structure was analyzed by X-ray diffraction (XRD, D8-Avance, Bruker, Germany) scanned in the range 10°–80° at 0.1° s^{-1}.

The Fourier transform infrared spectroscopy (FTIR) spectra were recorded with a Tensor 27 spectrometer using KBr pellets. Spectra in the range of 4000–400 cm^{-1} were obtained by 32 scans at a resolution of 4 cm^{-1}.

TG and derivative thermogravimetric analysis (DTG) were performed using a STA 449C thermal analyzer (Netzsch, Germany). About 7 mg of the specimens was heated from 20 to 800 °C at a linear heating rate of 10 °C min^{-1}. All runs were performed in N_2 at a flow rate of 50 mL min^{-1}.

The limit oxygen index (LOI) values were determined in accordance with ASTM standard D2863-2000 using a JF-3 oxygen index meter (Jiangning Analytical Instrument Factory, China). The specimens used for the test were of dimensions 100.0 × 6.5 × 3.0 mm^3.

Cone calorimetry was performed using a cone calorimeter (Fire Testing Technology Ltd., UK) according to ISO5660. Each specimen (100.0 × 100.0 × 3.0 mm^3) was wrapped in aluminum foil and exposed horizontally to a 50 kW m^{-2} external heat flux.

The tensile strength and elongation at break of the samples were tested using a tensile tester at a tensile rate of 200 mm min^{-1} according to the ISO527-2(1996). The size of the sample is 25.0 × 1.0 × 6.0 mm^3.

The samples were previously frozen at − 30 °C for 3 h, and then, the impact strength was measured by notched impact on a pendulum impact tester. The size of the spline is 50.0 × 4.0 × 5.0 mm^3.

Results and discussion

Structural characterization

Figure 1 shows the SEM image of four flame retardants M-CS. It can be seen from the figure that the four products are randomly flocculent. It is worth noting that the product has no obvious agglomeration and shows good dispersion. This may improve the mechanical properties of the flame-retardant polymer material to some extent.

Figure 2a shows the XRD pattern of the flame retardants. It can be seen that the XRD curves of the flame retardants are messy and disorderly, showing very low crystallinity, indicating that the flame retardants are disordered amorphous state. Combined with the SEM and XRD patterns, it can be concluded that the flame retardants M-CS all are amorphous precipitate.

The FTIR spectra of CS, Sn-CS, Mo-CS, Si-CS and W-CS are shown in Fig. 2b. The spectra reveal that abundant surface functional groups are present on CS. It can be seen that the wide band at 3433 cm^{-1} can be assigned to the stretching vibrations of –OH and $–NH_2$ [24]. At 2938 cm^{-1} and 2863 cm^{-1}, there are two absorption peaks generated by the stretching vibration of –C–H. The absorption peaks at 1628 cm^{-1} and 1590 cm^{-1} are attributed to the amide I (owing to the stretching vibration of C=O) and an amide II (owing to the deformation vibration of N–H) [25]. And, there is a strong absorption peak at 1086 cm^{-1} generated by asymmetric vibration of C–O–C [26]. Different from CS, the flame retardants all contain a stretching vibration peak corresponding to its acid radical. The peaks at 560, 880, 800 and 700–1000 cm^{-1} correspond to characteristic absorption peaks of Sn–O, M–O, Si–O and tungstate. And,

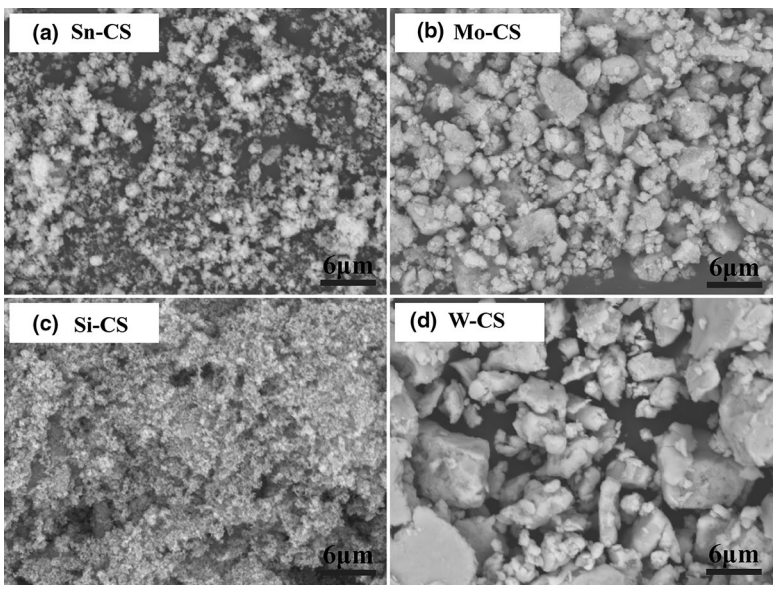

Fig. 1 SEM images of four flame retardants: Sn-CS (**a**), Mo-CS (**b**), Si-CS (**c**) and W-CS (**d**)

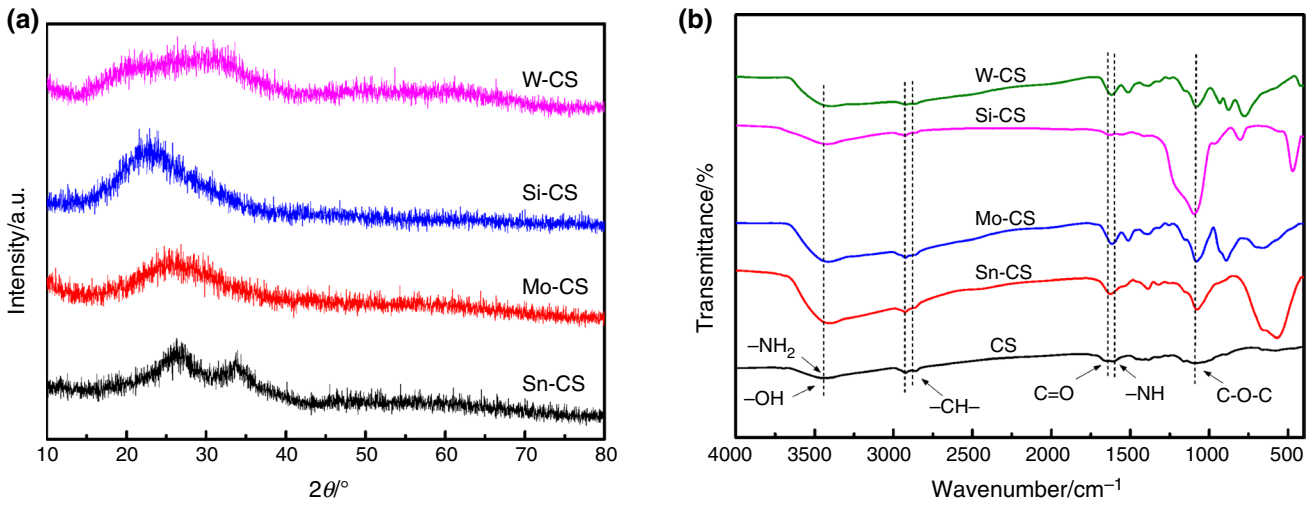

Fig. 2 XRD patterns (**a**) and FTIR spectra (**b**) of Sn-CS, Mo-CS, Si-CS and W-CS

it can be seen from the result that all the products have the basic structures of CS, from which it can be inferred that the inorganic salts all react with CS.

Thermal stability of flame retardant

TG analysis is an important means of characterizing the thermal stability of a test sample. We can get the mass change and the mass loss rate curve of the sample over the test temperature. Figure 3a shows the TG curves of the samples under a nitrogen atmosphere. It can be seen that the temperatures of 5% mass loss ($T_{5\ \mathrm{mass\%}}$) and the maximum mass loss rate ($T_{\max}$) of CS are 271.7 °C and 297.0 °C, respectively, and the residual rate of the sample is 35.53% at the temperature of 800 °C. The reaction with inorganic oxyacid salts has a significant effect on the thermal decomposition behavior of CS. The $T_{5\ \mathrm{mass\%}}$ and $T_{\max}$ of the flame retardants Sn-CS, Mo-CS, Si-CS and W-CS are significantly reduced compared to CS. It is worth noting that all of them have high residual rate of residues, with the values 71.34%, 41.18%, 83.40% and 71.51%, respectively. These results indicate that the flame retardants M-CS all have high residual rate under high temperature. At the same time, the sufficient thermal stability of the flame retardant can meet the processing temperature of engineering plastics, making it better used in polymer materials. From Fig. 3b, it can be seen that the residue of CS in the air atmosphere approaches zero. According to the residual amount of various flame retardants, the content of CS in Sn-CS, Mo-CS, Si-CS and W-CS can be roughly calculated as 9.6%, 48.3%, 13.5% and 22.6%, respectively. The higher CS content of Mo-CS is mainly due to the poor binding capacity of molybdate and CS, which can

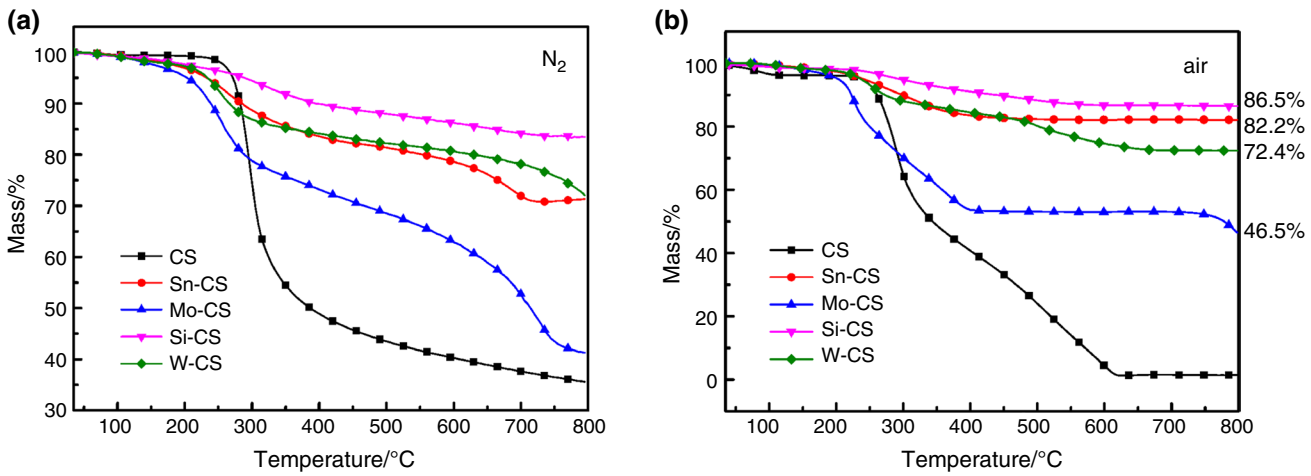

Fig. 3 TG curve of four flame retardants

also be seen from the low yield of Mo-CS. This result will reduce the flame-retardant performance of Mo-CS to a certain extent. In turn, the content of CS in the flame retardant also affects the thermal degradation behavior of the flame retardant. Mo-CS has the highest CS content, which leads to its early decomposition, and its residue is significantly less than other flame retardants.

Fire behavior

The LOI test is a traditional method to evaluate the flammability of flame-retardant materials. The results of the samples are presented in Table 1. As can be seen from Table 1, the pure PVC shows a certain flame retardancy with an LOI of 26.6% due to the addition of DOP and other additives. When Mo-CS, Si-CS and W-CS were added as flame retardants, the LOI value of PVC composites was improved to some extent compared with that of pure PVC. And it is worth noting that Sn-CS has superior performance. The LOI of the PVC/Sn-CS increases to 30.5%, which is 3.9% higher than that of the pure PVC. We can give a verdict that the introduction of Sn-CS has a certain flame-retardant effect on pure PVC.

Cone calorimetry test is considered to be an effective means of simulating the combustion of materials in a real environment, and it can provide some important combustion data and a comprehensive evaluation of the flame-retardant properties of the materials [27]. Heat release rate (HRR) is the main index of fire risk, and Fig. 4 shows the HRR curves of pure PVC, PVC/Sn-CS, PVC/Mo-CS, PVC/Si-CS and PVC/W-CS. It can be seen from Fig. 4 that the HRR of the pure PVC has two peaks and the PHRR is 297.49 kW m^{-2} and 232.12 kW m^{-2}, respectively. When Mo-CS and W-CS were added as flame retardants, there was no significant change in the PHRR of PVC composites, and the PHRR is 283.44 kW m^{-2} and 326.41 kW m^{-2}, respectively. This indicates that Mo-CS and W-CS do not play a good role in

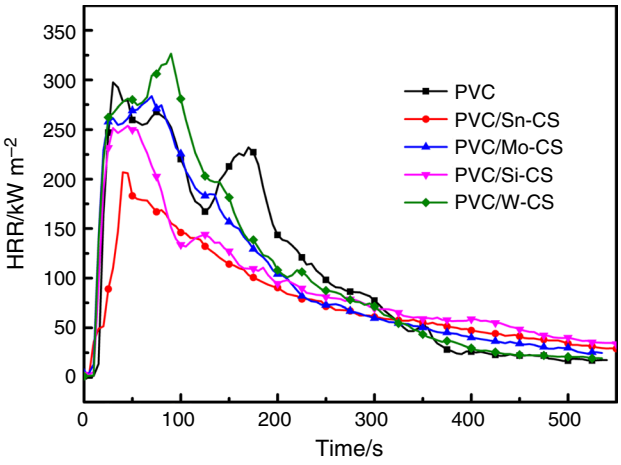

Fig. 4 HRR curves of PVC composites under a heat flux of 50 kW m^{-2}

reducing the HRR of the PVC materials, while it is worth noting that the PHRR of PVC composites decreased to 206.86 kW m^{-2} and 253.86 kW m^{-2} when adding Sn-CS and Si-CS as flame retardants. Compared with pure PVC, it decreased by 30.46% and 14.67%, respectively. Sn-CS shows the best performance among the four flame retardants. This phenomenon is mainly because stannate can catalyze the early decomposition of PVC and promote the carbonization of the product [28]. The carbonized product can effectively protect the polymer backbone and inhibit the transfer of heat and oxygen. In addition, the content of CS in Sn-CS is the lowest in the prepared flame retardant, which makes the content of flame-retardant element Sn higher than other flame retardants. For various reasons, Sn-CS has played a more efficient flame-retardant role.

Figure 5 shows the total heat release (THR) curve of PVC and its composites. As can be seen from Fig. 5, the THR curves of the PVC composite materials rise rapidly and tend

Table 1 Data of LOI and cone calorimeter tests for PVC composites

Sample	PVC	PVC/Sn-CS	PVC/Mo-CS	PVC/Si-CS	PVC/W-CS
LOI/%	26.6	30.5	26.8	26.3	27.0
TTI/s	20	11	16	17	16
PHRR/kW m^{-2}	297.49	206.86	283.44	253.86	326.41
t_{PHRR}/s	30	40	70	45	90
THR/MJ m^{-2}	58.30	47.67	54.66	53.72	58.24
PSPR/m^2 s^{-1}	0.1980	0.1011	0.1656	0.2256	0.1821
TSP/m^2	28.26	13.41	19.60	22.43	21.17
Av-EHC/MJ kg^{-1}	14.56	12.93	14.58	14.74	15.11
Av-SEA/m^2 kg^{-1}	789.37	403.89	576.49	690.42	584.80
Av-COY/kg kg^{-1}	0.1070	0.1353	0.0993	0.0945	0.0954
Av-CO2Y/kg kg^{-1}	0.8863	0.7510	0.9125	0.8993	0.9560
Residue/%	4.74	17.90	13.39	12.12	10.76

to be stable at 500 s. The pure PVC has a high THR with a value of 58.30 MJ m^{-2}. Unlike pure PVC, the THR values of PVC composites rise slowly when flame retardants are added. After burning for 500 s, the PVC/Sn-CS, PVC/Mo-CS and PVC/Si-CS all have a lower THR, whose values were 47.67 MJ m^{-2}, 54.66 MJ m^{-2} and 53.72 MJ m^{-2}, respectively. We can know from the results that Sn-CS can more effectively reduce the heat release of PVC composites. This is mainly because stannate promotes the formation of char layers and prevents the release of heat, which can effectively inhibit the burning of PVC in real fire.

In addition to heat release, another hazard associated with burning PVC is the smoke produced during combustion. The smoke production rate (SPR) and total smoke production (TSP) are used to evaluate the smoke suppression performance of PVC composites. It can be seen from Fig. 6 that the SPR of pure PVC has a high peak and reaches a maximum after 25 s of ignition, and the value of PSPR (peak smoke production rate) is 0.198 m^2 s^{-1}. When the flame retardants are added, the SPR of the PVC composite materials changes a lot. The SPR values of PVC/Sn-CS, PVC/Mo-CS, PVC/Si-CS and PVC/W-CS rise rapidly after combustion and reach the maximum, which may be due to the fact that the addition of flame retardant promotes the early decomposition of the material, resulting in the rapid release of smoke. However, as the combustion progresses, the smoke released by the flame-retardant PVC is rapidly reduced and is much less than pure PVC. Sn-CS exhibits excellent performance in suppressing the release of smoke from PVC composites, in both the early and late stages of combustion, and the PSPR value of PVC/Sn-CS is only 0.101 m^2 s^{-1}, which is 48.99% lower than that of pure PVC. The decrease in the SPR value indicates that the amount of smoke generated by the burning of the material per unit time is reduced, which can effectively lower the density of smoke in the unit space and reduce the casualties caused by smoke poisoning in the event of fire.

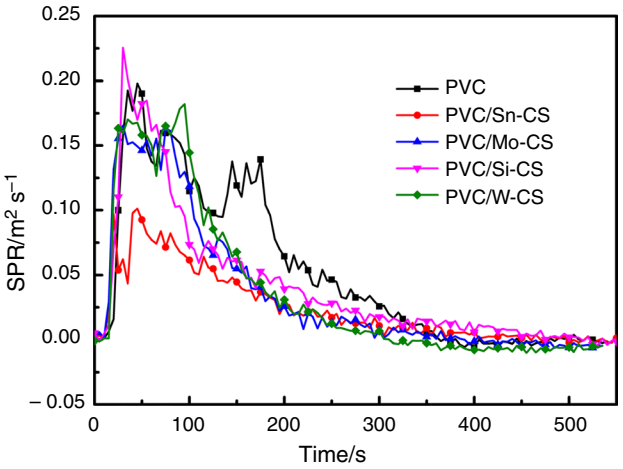

Fig. 6 SPR curves of PVC composites under a heat flux of 50 kW m^{-2}

Figure 7 shows the TSP curve of the sample after the cone test. We can see from Fig. 7 that the TSP curves of all samples show a linear growth trend in the initial stage and remain stable after 300 s. Combining Fig. 7 and Table 1, we can find that the TSP value of pure PVC is 28.26 m^2 which is much higher than that of the flame-retardant PVC sample. PVC/Sn-CS has the lowest TSP in all samples, with a value of 13.41 m^2, which is 52.55% lower than pure PVC. At the same time, the TSP values of PVC/Mo-CS, PVC/Si-CS and PVC/W-CS were reduced to 19.60 m^2, 22.43 m^2 and 21.17 m^2, respectively. Compared with pure PVC, the smoke suppression performance has been greatly improved. From

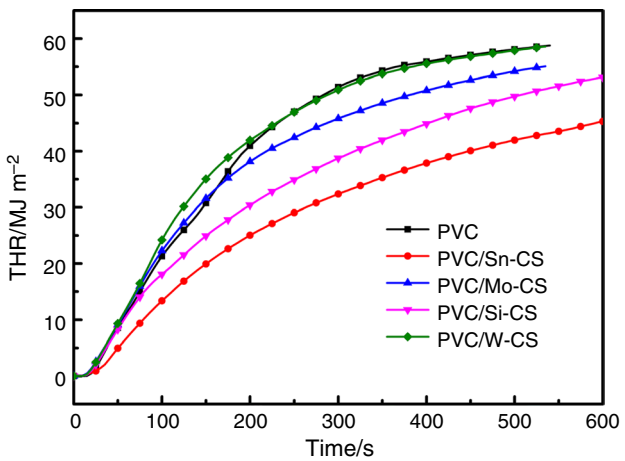

Fig. 5 THR curves of PVC composites under a heat flux of 50 kW m^{-2}

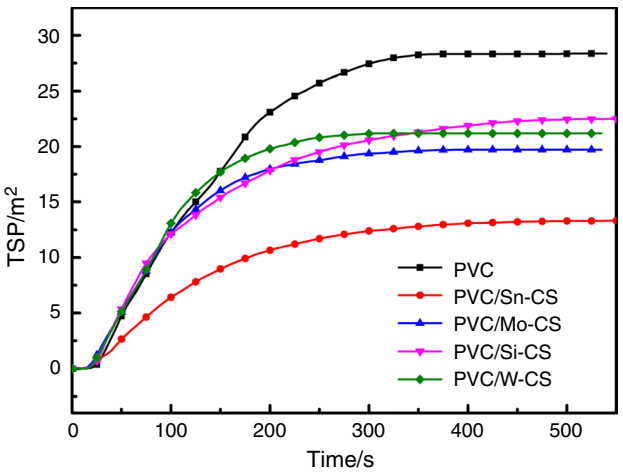

Fig. 7 TSP curves of PVC composites under a heat flux of 50 kW m^{-2}

the result, we can find that PVC/M-CS has good smoke suppression performance after adding ten parts of M-CS.

Thermal stability of PVC and its composites

In order to investigate the thermal degradation properties of PVC composites, TG and DTG tests were performed on PVC samples under nitrogen atmosphere. The results are shown in Fig. 8 and Table 2.

The thermal degradation of PVC composites is divided into two stages. The first stage is in the vicinity of 200–350 °C, corresponding to the decomposition of DOP and the removal of hydrogen chloride (HCl) [29]. The second stage is around 420–530 °C due to the cross-linking of the C=C bond and the further oxidation of the unstable char residue. For pure PVC, the $T_{5\ mass\%}$ is 255 °C and the R_{max} is 12.32% min^{-1}. The addition of flame retardant has a great influence on the thermal degradation of PVC. Compared with pure PVC, the $T_{5\ mass\%}$ of the four flame-retardant PVC composites has a certain reduction. It is worth noting that the R_{max} of PVC/Sn-CS composite is 53.36% min^{-1} in the first degradation stage, which is much higher than that of pure PVC. In addition, the T_{max} of PVC/Sn-CS is 255.7 °C, which is much lower than that of other samples. This showed that Sn-CS can catalyze the early thermal degradation of PVC materials and promote their cross-linking into char. This result can be explained by the reaction of tin with the hydrogen chloride emitted from PVC to generate tin chloride (a strong Lewis acid), which catalyzes the decomposition of PVC and enhances its early cross-linking. At the same time, the release of HCl during the degradation process helps to improve the self-extinguishing performance of the material, which corresponds to the LOI value of PVC composites in the LOI test results. The thermal decomposition rate of PVC/Sn-CS in the first stage is significantly greater than that of other samples, giving it the maximum value of LOI.

Table 2 TG and DTG data for PVC composites at 10 °C min^{-1} under nitrogen atmosphere

Sample	$T_{5\%}$/°C	R_{max}/% min^{-1}	T_{max}/°C	Residue at 800 °C/mass%
PVC	255.1	− 12.32	311.1	10.53
PVC/Sn-CS	252.3	− 53.36	255.7	16.90
PVC/Mo-CS	254.0	− 21.13	274.9	19.67
PVC/Si-CS	251.8	− 10.95	311.6	15.24
PVC/W-CS	253.3	− 12.05	303.7	17.23

In the second stage, the maximum mass loss rate of the four flame-retardant PVC composites and the temperature corresponding to the maximum mass loss rate are substantially the same as those of pure PVC. However, the residual quality of the flame-retardant PVC is greatly increased. The char residue rates of PVC/Sn-CS, PVC/Mo-CS, PVC/Si-CS and PVC/W-CS were 16.90%, 19.67%, 15.24% and 17.23%, respectively, which were increased by 60.49%, 86.80%, 44.73% and 63.63%, respectively, compared with pure PVC. This indicates that the stability of the char residual of the flame-retardant PVC composites is improved, resulting in an increase in the amount of char residue. The increase in char residue effectively improves the thermal insulation properties and the oxygen barrier properties of the material, thereby improving the flame-retardant and smoke-suppressing properties of the material. It is worth noting that the PVC/Sn-CS gives the material the best flame-retardant properties even its char residue is not the most. However, it can be seen from the microscopic morphology that the surface of the char residue of the PVC/Sn-CS is denser, showing the

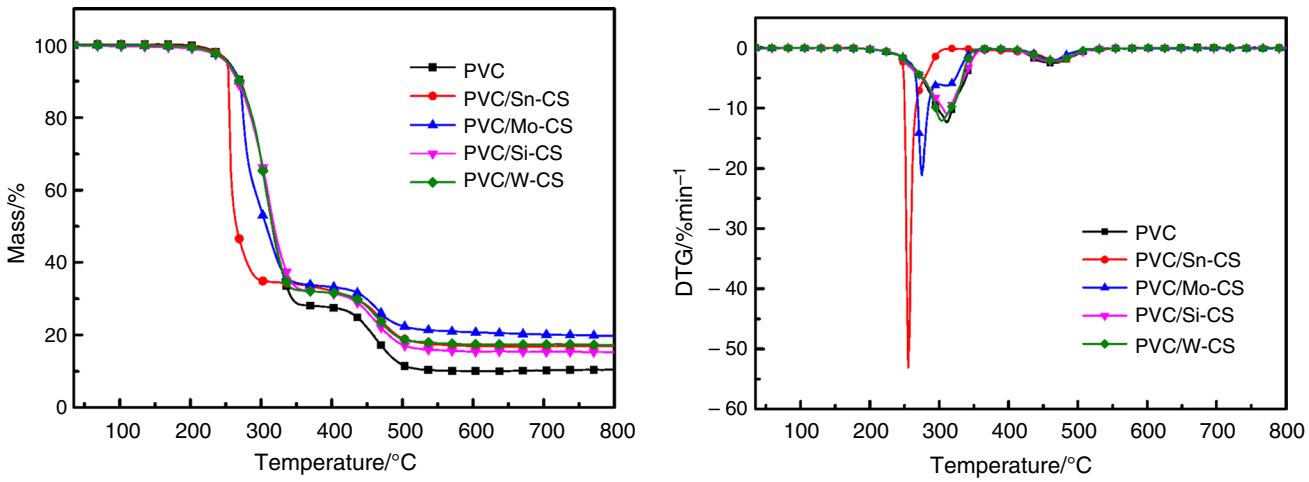

Fig. 8 TG and DTG curves of PVC composites

high-efficiency catalytic char formation of tin. In addition, it can be found that the char residue of PVC material is slightly different from the cone test results. This is mainly because the TG test of PVC materials is carried out in a nitrogen atmosphere, which makes the activity of the flame retardant suppressed to a certain extent so that the gap between the flame retardants is reduced. In this case, even the amount of char residue in PVC/Mo-CS slightly exceeds PVC/Sn-CS. Mo-CS with lower Mo content has a higher char residue rate, which also shows that Mo has better char-forming ability.

Char residue analysis

The surface morphologies of the char residues gathered after LOI test were studied by SEM. The SEM micrographs are shown in Fig. 9. The char residue of the pure PVC matrix is loose, and the char layer is cracked and has many voids. This indicates that pure PVC is thermally degraded after ignition and volatilizes a large amount of flammable gas. These gases can break through the char layer and form a large number of voids on the surface of the char residue. In addition, these gases will burn intensely when in contact with air, causing an increase in fire. Violent fire also creates an updraft that causes the charcoal to float into the air and form a large amount of soot. Unlike other flame-retardant PVC composites, the char residual of PVC/Si-CS loosens and expands. This may be caused by the inertness of the silicate. The reason for this phenomenon is that the silicate will decompose to form a relatively stable silicon-containing oxide at high temperature, which can play a certain physical filling role. Moreover, this oxide is rigid and fragile and will break into fluffy powdery substance during its temperature drop from high temperature [30]. In addition, a large amount of gas was generated during the pyrolysis of the composite, which can cause the residue to expand to some extent, while the surfaces of char residue of PVC/Sn-CS, PVC/Mo-CS and PVC/W-CS are dense and have no obvious cracks and pores. A certain amount of irregular white small particles is evenly distributed on the surface of the char layer, which can be presumed to be chlorides and oxides produced during the combustion process. This indicates that the flame retardant can promote cross-linking of the PVC composite into char during the combustion process and form a dense protective layer. The char layer prevents the substrate from coming into contact with flammable gases, thereby improving the flame-retardant properties of the material.

Figure 10 shows the XRD pattern of the char residual of the PVC composite after cone calorimetry test. It can be seen from Fig. 10 that the peak corresponding to PVC is width and gentle which is attributed to the fact that the PVC residual is amorphous. The diffraction peak of PVC/Sn-CS is consistent with the standard card of SnO_2(PDF#41-1445). The diffraction peak of PVC/Mo-CS is consistent with the standard map of MoO_3(PDF#65-5787). These results demonstrate the formation of oxides of flame-retardant elemental during combustion, and this also explains the good catalytic properties of the flame retardants to some degree.

Mechanical performance analysis

Mechanical tests include tensile testing and impact testing to characterize the mechanical properties of composites. The mechanical properties of the material are related to the shape and structure of the particles and their distribution

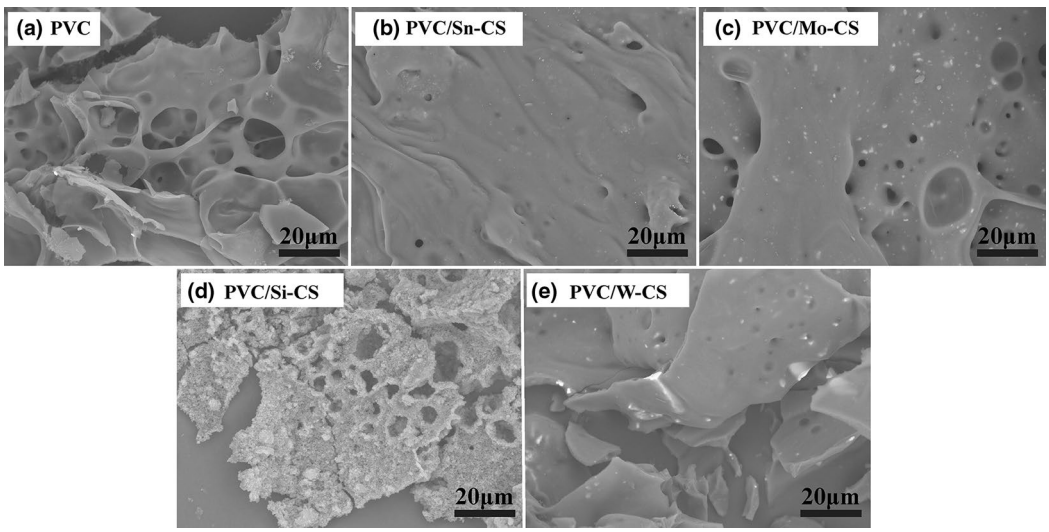

Fig. 9 SEM images of char residues for samples after LOI: PVC (**a**), PVC/Sn-CS (**b**), PVC/Mo-CS (**c**), PVC/Si-CS (**d**) and PVC/W-CS (**e**)

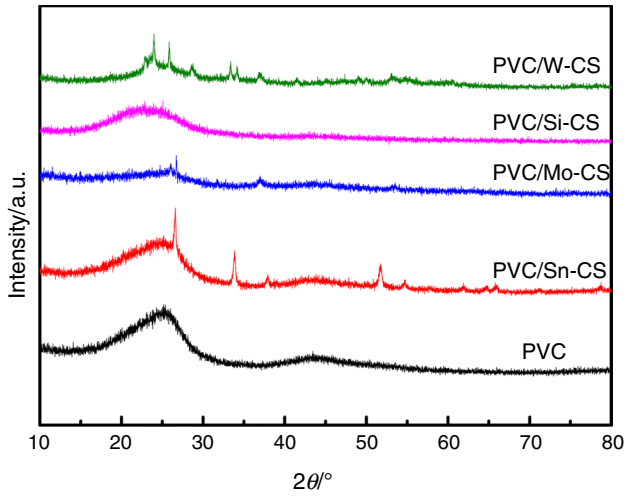

Fig. 10 XRD patterns of char residue of PVC and PVC composites after CONE test

in the polymer matrix and the intermolecular interaction between the particles and the polymer matrix. The tensile testing and impact testing results and curves are given in Table 3. It can be seen that the elongation at break of pure PVC is 447.54%, the tensile strength is 23.35 MPa, and the impact strength is 1.81 kJ m^{-2}. According to previous experiments, the addition of 5 phr traditional flame-retardant Sb_2O_3 reduced the elongation at break of PVC materials by 36% [31]. Compared with Sb_2O_3, the addition of chitosan-based flame retardants can significantly reduce the adverse effects of flame retardants on the elongation at break of PVC materials. The elongation at break of PVC/Sn-CS, PVC/Mo-CS, PVC/Si-CS and PVC/W-CS is 394.74%, 427.01%, 371.70% and 419.18%, respectively, which decrease only by 11.80%, 4.59%, 16.95% and 6.34%, respectively, compared with that of pure PVC. This is mainly because the $–NH_2$ in chitosan is a reactive group that can lose electrons. When NH_2 encounters a strong electron-withdrawing functional group –Cl, there is a weak interaction between them. A large amount of such bonding can form a cross-linked network to improve the compatibility between the chitosan-based flame retardant and the PVC substrate, thereby improving the mechanical properties of the PVC material [32–34].

In addition, the addition of flame retardant effectively improves the impact resistance of PVC composites. Compared with pure PVC, the impact strength of PVC/Sn-CS, PVC/Mo-CS, PVC/Si-CS and PVC/W-CS increased by

Table 3 Tensile and impact resistance data of PVC and its composites

Sample	Elongation at break/%	Tensile strength/MPa	Impact strength/kJ m^{-2}
PVC	447.54 ± 2.30	23.35 ± 0.24	1.81 ± 0.19
PVC/Sn-CS	394.74 ± 9.79	21.45 ± 0.60	2.69 ± 0.25
PVC/Mo-C	427.01 ± 7.06	18.82 ± 0.56	2.45 ± 0.13
PVC/Si-CS	371.70 ± 7.30	22.41 ± 0.37	2.62 ± 0.20
PVC/W-CS	419.18 ± 5.16	20.63 ± 0.84	2.17 ± 0.17

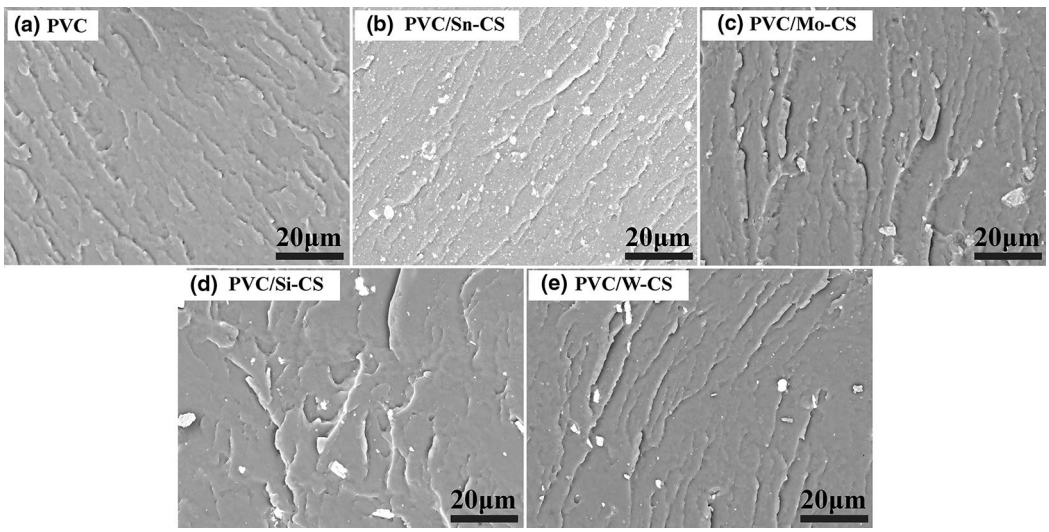

Fig. 11 SEM images of the PVC composites sections: PVC (**a**), PVC/Sn-CS (**b**), PVC/Mo-CS (**c**), PVC/Si-CS (**d**) and PVC/W-CS (**e**)

48.62%, 35.36%, 44.75% and 19.86%, respectively. This is due to the increased interaction between the CS and the PVC matrix, which reduces the shear between the flame retardant and the matrix during impact. At the same time, the addition of an appropriate number of rigid particles can effectively absorb the impact energy, thereby enhancing the impact resistance of the material.

Impact section analysis

The compatibility and dispersion of the flame retardant in the collective can be studied by analyzing the cross section of the sample. The impact section of PVC and its composites is shown in Fig. 11. The interface of the pure PVC section is relatively flat and smooth, and the cracks generated during the fracture are evenly distributed on the section. Compared with pure PVC, the cross sections of PVC/Sn-CS, PVC/Mo-CS, PVC/Si-CS and PVC/W-CS are relatively rough, indicating that the polyhydroxy structure of CS can react with the PVC matrix. The flame retardants are evenly distributed on the cross section, and no obvious agglomeration occurred. This demonstrates good compatibility between the flame retardant and the PVC matrix. This good compatibility also explains the improvement in the mechanical properties of flame-retardant PVC composites.

Conclusions

In this work, chitosan-regulated inorganic oxyacid salt flame retardants including PVC/Sn-CS, PVC/Mo-CS, PVC/Si-CS and PVC/W-CS were prepared and used into PVC composites to improve the flame-retardant and smoke-suppressing properties of materials while improving the mechanical properties of the materials. Compared to the other three flame retardants, Sn-CS shows the best performance in terms of LOI. The LOI value of Sn-CS reached 30.5%. In addition, the incorporation of Sn-CS in the cone calorimetry test resulted in a significant decrease in heat release rate, total heat and smoke release, and mass loss rate. The addition of four flame retardants can increase the amount of char residue in the PVC composite. Among them, Sn-CS and Mo-CS can catalyze the removal of HCl from PVC, accelerate the carbonization process and generate a stable char layer during the combustion of the substrate. In addition, the addition of flame retardant had little effect on the tensile properties of PVC composites, but its impact resistance had been greatly improved. In summary, the M-CS flame retardant obtained in the experiment can not only improve the flame retardancy of PVC, but also improve the mechanical properties of the substrate. This bio-based flame retardant is a new type of green high-efficiency flame retardant, which deserves further study.

Acknowledgements This work was supported by the Higher Education Science and Technology Research Project of Hebei Province [Grant Number ZD2018011]; the Key Basic Research Project of Hebei Province [Grant Number 16961402D]; and the Key Research Project of Hebei Province [Grant Number 19211205D].

References

1. Sun YJ, Gao M, Chai ZH, Wang H. Thermal behavior of the flexible polyvinyl chloride including montmorillonite modified with iron oxide as flame retardant. J Therm Anal Calorim. 2018;131(1):65–70.
2. Li M, Xia JL, Ding HY, Ding CX, Wang M, Li SH. Optimal design, characterization, and thermal stability of bio-based Ca/Na/Zn composite stabilizer derived from myrcene for poly(vinyl chloride). Polym Degrad Stab. 2017;139:117–29.
3. Yu J, Sun L, Ma C, Qiao Y, Yao H. Thermal degradation of PVC: a review. Waste Manag. 2016;48:300–14.
4. Wu WH, Wu HJ, Liu WH, Wang YE, Liu N, Yang XM, Li YM, Qu HQ. Two series of inorganic melamine salts as flame retardants and smoke suppressants for flexible PVC. Polym Compos. 2018;39(2):529–36.
5. Yin Z, Chen K, Wang HJ, Wang HY, Wei Z. Mechanical properties, flame retardancy, and smoke suppression of lanthanum organic montmorillonite/poly(vinyl chloride) nanocomposites. J Appl Polym Sci. 2016;133(39):43951.
6. Hirschler MM. Poly(vinyl chloride) and its fire properties. Fire Mater. 2017;41(8):993–1006.
7. Coaker AW. Fire and flame retardants for PVC. J Vinyl Addit Technol. 2003;9(3):108–15.
8. Xu JZ, Liu CH, Qu HQ, Ma HY, Jiao YH, Xie JX. Investigation on the thermal degradation of flexible poly(vinyl chloride) filled with ferrites as flame retardant and smoke suppressant using TGA-FTIR and TGA-MS. Polym Degrad Stab. 2013;98(8):1506–14.
9. Yu JC, Xu AW, Zhang LZ, Song RQ, Wu L. Synthesis and characterization of porous magnesium hydroxide and oxide nanoplates. J Phys Chem B. 2004;108(1):64–70.
10. Chang SK, Zeng C, Yuan WZ, Ren J. Preparation and characterization of double-layered microencapsulated red phosphorus and its flame retardance in poly(lactic acid). J Appl Polym Sci. 2012;125(4):3014–22.
11. Fei G, Wang Q, Liu Y. Synthesis of novolac-based char former: silicon-containing phenolic resin and its synergistic action with magnesium hydroxide in polyamide-6. Fire Mater. 2010;34(8):407–19.
12. Fang SL, Hu Y, Song L, Zhan J, He QL. Mechanical properties, fire performance and thermal stability of magnesium hydroxide sulfate hydrate whiskers flame retardant silicone rubber. J Mater Sci. 2008;43(3):1057–62.
13. Kum CH, Cho Y, Joung YK, Choi J, Park K, Seo SH, Park YS, Ahn DJ, Han DK. Biodegradable poly(L-lactide) composites by oligolactide-grafted magnesium hydroxide for mechanical reinforcement and reduced inflammation. J Mater Chem B. 2013;1(21):2764–72.
14. Song QY, Wu HJ, Liu H, Han XX, Qu HQ, Xu JZ. Synergistic flame-retardant effects of ammonium polyphosphate and AC-Fe_2O_3 in epoxy resin. J Therm Anal Calorim. 2019;138(2):1259–76.

15. Jiang WJ, Hua XF, Han QF, Yang XJ, Lu LD, Wang X. Preparation of lamellar magnesium hydroxide nanoparticles via precipitation method. Powder Technol. 2009;191(3):227–30.
16. Meng WH, Wu WH, Zhang WW, Cheng LY, Han XX, Xu JZ, Qu HQ. Bio-based $Mg(OH)_2$@M-Phyt: improving the flame-retardant and mechanical properties of flexible poly(vinyl chloride). Polym Int. 2019;68(10):1759–66.
17. Zhang B, Jiang YJ, Han J. Synthesis of zinc stannate microcapsules for preparation of flame-retardant PVC composites. Polym Plast Technol. 2018;57(12):1242–53.
18. Wang ZZ, Haung ZY, Li XY, Zhou JA. A nano graphene oxide/alpha-zirconium phosphate hybrid for rigid polyvinyl chloride foams with simultaneously improved mechanical strengths, smoke suppression, flame retardancy and thermal stability. Compos Part A Appl S. 2019;121:180–8.
19. Nama S, Condon BD, Xia ZY, Nagarajan R, Hinchliffe DJ, Madison CA. Intumescent flame-retardant cotton produced by tannic acid and sodium hydroxide. J Anal Appl Pyrol. 2017;126(1):239–46.
20. Pires NR, Cunha PLR, Maciel JS, Angelim AL, Melo VMM, de Paula RCM, Feitosa JPA. Sulfated chitosan as tear substitute with no antimicrobial activity. Carbohydr Polym. 2013;91(1):92–9.
21. Lawrie G, Keen I, Drew B, Chandler-Temple A, Rintoul L, Fredericks P, Grondahl L. Interactions between alginate and chitosan biopolymers characterized using FTIR and XPS. Biomacromolecules. 2007;8(8):2533–41.
22. Suh JK, Matthew HW. Application of chitosan-based polysaccharide biomaterials in cartilage tissue engineering: a review. Biomaterials. 2000;21(24):2589–98.
23. Zhang T, Yan HQ, Shen L, Fang ZP, Zhang XM, Wang JJ, Zhang BY. Chitosan/phytic acid polyelectrolyte complex: a green and renewable intumescent flame retardant system for ethylene-vinyl acetate copolymer. Ind Eng Chem Res. 2014;53(49):19199–207.
24. Staroszczyk H, Sztuka K, Wolska J, Wojtasz-paja A, Kolodziejska I. Interactions of fish gelatin and chitosan in uncrosslinked and crosslinked with EDC films: FT-IR study. Spectrochim Acta A. 2014;117:707–12.
25. Qiao CD, Ma XG, Zhang JL, Yao JS. Molecular interactions in gelatin/chitosan composite films. Food Chem. 2017;235:45–50.
26. Wang XH, Li DP, Wang WJ, Feng QL, Cui FZ, Xu YX, Song XH, van der Werf M. Crosslinked collagen/chitosan matrix for artificial livers. Biomaterials. 2003;24(19):3213–20.
27. Gangireddy CSR, Wang X, Kan YC, Song L, Hu Y. Synthesis of a novel DOPO-based polyphosphoramide with high char yield and its application in flame-retardant epoxy resins. Polym Int. 2018;68(5):936–45.
28. Qu HQ, Wu WH, Jiao YH, Xu JZ. Thermal behavior and flame retardancy of flexible poly(vinyl chloride) treated with $Al(OH)_3$ and ZnO. Polym Int. 2005;54(11):1469–73.
29. Wang ZZ, Huang ZY, Li XY, Zhou JA. A nano graphene oxide/α-zirconium phosphate hybrid for rigid polyvinyl chloride foams with simultaneously improved mechanical strengths, smoke suppression, flame retardancy and thermal stability. Compos Part A Appl Sci Manuf. 2019;121:180–8.
30. Wu WH, Leng JJ, Wang Z, Qu HQ, Gao JG. Preparation, curing, and properties of boron-containing bisphenol-S formaldehyde resin/o-cresol formaldehyde epoxy resin/nano-SiO_2 composites. Macromol Res. 2016;24(3):209–17.
31. Pan YT, Wang DY. Fabrication of low-fire-hazard flexible poly (vinyl chloride) via reutilization of heavy metal biosorbents. J Hazard Mater. 2017;339:143–53.
32. Zhu XY, Hou XL, Ma BM, Xu HL, Yang YQ. Chitosan/gallnut tannins composite fiber with improved tensile, antibacterial and fluorescence properties. Carbohyd Polym. 2019;226:115311.
33. Yang XM, Li YY, Wang YL, Yang YG, Hao JW. Nitrocellulose-based hybrid materials with T7-POSS as a modifier: effective reinforcement for thermal stability, combustion safety, and mechanical properties. J Polym Res. 2017;24(3):50.
34. Yang X, Meng NN, Zhu YC, Zhou YF, Nie WY, Chen PP. Greatly improved mechanical and thermal properties of chitosan by carboxyl-functionalized MoS_2 nanosheets. J Mater Sci. 2016;51(3):1344–53.